Gasflow style level posture sensor and angular velocity gyroscope assembled inertial sensor*

Zhang Fuxue** and Mao Xu

(Research Centre of Sensor Technology, Beijing Information Technology Institute, Beijing 100101, China)

Accepted on February 8, 2007

Abstract The compensational loop consisting of a gasflow style angular velocity gyroscope and gasflow level posture sensor is proposed to improve the signal of gasflow style tilt. This compensational loop could remove acceleration interfere from the signal of tilt. This assembled gasflow type inertial sensor not only measures static state angular, but also restrains the acceleration which interferes the output signal of level posture sensor in dynamic situations. Therefore, the precision of outputs signal increases greatly. Moreover, the output signal includes the angle velocity signal.

Keywords: gasflow style, inertia, sensor.

The common tilt can be measured accurately without the interfere of acceleration, but the interfere of the acceleration introduces errors under the dynamic condition[1,2].

At present, level posture of an object can be measured by a compensational loop equipment that has a clinometer (solid type pendulum or liquid type pendulum tilt sensor) and rate gyroscope, but this equipment is expensive, with long response time and the feebleness of resistant vibration.

In order to avoid the effect of the acceleration, we developed a compensational loop equipment that was constituted by a gasflow type angle rate gyroscope and a gasflow type level posture sensor, removing the interfere of the acceleration by the gyroscope signal. This assembled gasflow style inertial sensor not only measures static state angular, but also restrains the acceleration which interferes the output signal of level posture sensor in dynamic situation. Because all the proof mass of the gasflow type angle rate gyroscope and the gasflow type level posture sensor is gas[3—5], the assemble inertial sensor has the capability of high impact resistance, low cost, and short response time.

1 Sense mechanisms

The gasflow style assemble inertial sensor consists of the signal circuits, the gasflow type angle rate gyroscope and the gasflow type level posture sensor. It can remove interference of the acceleration by the gyroscope signal and improve the measurement of obliquity to a high accuracy in dynamic situation.

1.1 Working principle of the gasflow style level posture sensor

Level posture sensor of gasflow style work mechanism was discussed in Ref. [5]. The natural convection gas has the pendulum property in the hermetic chamber. There are heat source and two sense arms on the electric bridge sense wires of heat in the hermetic chamber[5]. When the sensor is laid horizontally, the heat gas runs perpendicularly to the plane of the two impedance thermal resistance wires, the amounts of heat absorbed by thermal resistance wires are the same for the same temperature and so the bridge is balanced. When the sensor tilts, the heat gas runs perpendicular upward too, but it diverges the plane normal direction of thermal resistance wire, and different amount of heat was absorbed by the two thermal resistance wires at different temperatures, hence resistance values of the two thermal resistor wires are different, which will cause the imbalanced electric bridge, and output a voltage that is directly proportional to the tilt angle.

1.2 Work mechanism of the gasflow style angular velocity gyroscope

The gasflow style angular velocity gyroscope

* Supported by National Natural Science Foundation of China (Grant No. 60472011), and Beijing Key Laboratory for Sensor (No. 53062017)
** To whom correspondence should be addressed. E-mail: zhangfuxue@263.net

measures the angular velocity based on the principle that the gasflow diverges the movement curve under the Coriolis force. The gasflow bunch of the convection gasflow is driven by the piezoelectricity pump (velocity is V_j). As shown in Fig. 1, when angular velocity is ω_i, the gas layer flow bunch diverges the middle curve by Coriolis force, then the change of gasflow will affect the thermal resistance wire r_1 (or r_2). The resistance of thermal resistance wire is changed by the gasflow cooling, causing the electric bridge imbalanced and outputting a voltage V_0 directly proportional to angular velocity. The value and the orientation of the gasflow diverge determine the vector of the additional angular velocity. If the departure is Y, the Coriolis acceleration is

$$\ddot{Y} = 2\omega_i V_j \tag{1}$$

From Eq. (1), the velocity and bias of the gasflow are

$$\dot{Y} = 2\omega_i V_j t \tag{2}$$

$$Y = \omega_i V_j t^2 \tag{3}$$

If the distance between the thermal resistance wire and the spray head is L, then

$$L = V_j t \tag{4}$$

Substituting (4) into (2) and (3), then

$$\dot{Y} = 2\omega_i L \tag{5}$$

$$Y = \omega_i L t \tag{6}$$

As can be seen from (5), the gas flow velocity $\dot{Y}$ is directly proportional to angle velocity ω_i.

As can be seen from Fig. 1, the angular velocity signal can be gained from two parallel distributing thermal resistance sense wires. The two thermal resistance wires form two arms of the electric bridge. The velocity of the gasflow bunch is different, hence the output voltage of the electric bridge is also different. Moreover, when the angular velocity orientation is different, V_j is different too, thereby angular velocity orientation can be derived from the different effects on the two thermal resistance wires.

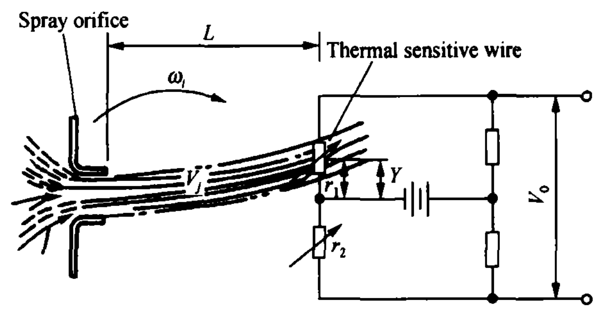

Fig. 1. Work mechanism of the gasflow style angular velocity gyroscope.

1.3 Working principle of the gasflow style assemble inertial sensor

A gasflow style tilt and an angular velocity gyroscope constitute the compensational loop which avoids the interfere of acceleration to improve the level posture sensor signal by the gyroscope signal. This sensor's working principle is shown in Fig. 2. The magnified output signal of level posture sensor $V_{I\theta}$ is inputted into the differentiator, and the output signals of the differentiator and the gasflow style angular velocity are inputted into the comparator A at the same time, so the output signal of comparator A is the interference signal of acceleration, then this signal is transmitted to the integrator. The voltage V_a' of filter and time-lapse output signal of the amplifer are provided to comparator B, thus getting the tilt angle signal which restrains the interfere of acceleration. Besides, the gasflow style angular velocity gyroscope can measure the angle velocity signal V_ω.

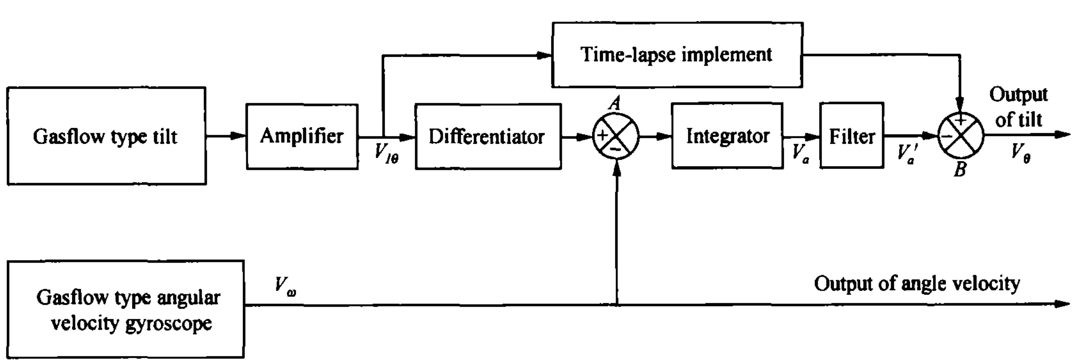

Fig. 2. Working principle of the Gasflow style assembled inertial sensor work mechanism.

Let the sensor move time be $[T_0, T_1]$, and insert $n-1$ time point into the move time

$$T_0 = t_0 < t_1 < \cdots < t_{n-1} < t_n = T_1 \quad (7)$$

then the $[T_0, T_1]$ include n small parts

$$[t_0, t_1], [t_1, t_2], \cdots, [t_{i-1}, t_i], \cdots, [t_{n-1}, t_n] \quad (8)$$

Let the small part be t, then

$$\Delta t_i = t_i - t_{i-1} = t \quad (9)$$

Let the angle velocity be ω_i in $[T_0, T_i]$, and the sense tilt angles be $\theta_0', \theta_1', \theta_2', \cdots, \theta_n'$ at $t_0, t_1, t_2, \cdots, t_n$, then the average velocity of the number small part i is

$$\omega_{\theta i} = \frac{\theta_i' - \theta_{i-1}'}{t} \quad (10)$$

Comparing (10) with the angle velocity of the number small part i, we have

$$\Delta\omega_i = \omega_{\theta i} - \omega_i = \frac{\theta_i' - \theta_{i-1}'}{t} - \omega_i \quad (11)$$

thus the tilt angle caused by acceleration in this small part is

$$\Delta\theta_{ai} = \Delta\omega_i \cdot t = (\theta_i' - \theta_{i-1}') - \omega_i t \quad (12)$$

So the sum of the tilt angle caused by acceleration in move time $[T_0, T_i]$ is

$$\theta_a = \sum_{i=1}^{n} \theta_{ai} = \sum_{i=1}^{n} [(\theta_i' - \theta_{i-1}') - \omega_i \cdot t] \quad (13)$$

thus the actual angle of the sensor is

$$\theta = \theta_n' - \theta_a \quad (14)$$

Substituting (13) into (14), we have

$$\theta = \theta_0' + \omega_i \cdot t \cdot n \quad (15)$$

Because there is no interfere at t_0

$$\theta_0' = \theta_0 \quad (16)$$

where $\theta_0$is the actual angle of the sensor at t_0.

Substituting (16) into (15), we have

$$\theta = \theta_0 + \omega_i \cdot t \cdot n \quad (17)$$

Let the output of sensor be the magnified voltage form, the tilt angle and angular velocity are expressed by

$$V_\theta = V_{0_\theta} + K_\theta \theta \quad (18)$$

$$V_\omega = V_{0_\omega} + K_\omega \omega_i \quad (19)$$

where V_{0_θ} and V_{0_ω} are the bias of tilt angle and angular velocity, K_θ and K_ω are the scale coefficient of tilt angle and angular velocity respectively.

From Eqs. (18) and (19) we have

$$\theta = \frac{V_\theta - V_{0_\theta}}{K_\theta} \quad (20)$$

$$\omega_i = \frac{V_\omega - V_{0_\omega}}{K_\omega} \quad (21)$$

$$\theta_0 = \frac{V_{\theta_0} - V_{0_\theta}}{K_\theta} \quad (22)$$

where V_{θ_0} is the output voltage of tilt angle θ_0 at t_0.

Substituting Eqs. (20)—(22) into (17), then

$$\frac{V_\theta - V_{0_\theta}}{K_\theta} = \frac{V_{\theta_0} - V_{0_\theta}}{K_\theta} + \frac{V_\omega - V_{0_\omega}}{K_\omega} \cdot t \cdot n \quad (23)$$

multiplying K_θ, then

$$V_\theta = V_{\theta_0} + (V_\omega - V_{0_\omega}) \cdot \frac{K_\theta}{K_\omega} \cdot t \cdot n \quad (24)$$

If

$$\frac{K_\theta}{K_\omega} = m \quad (25)$$

then

$$V_\theta = V_{\theta_0} + (V_\omega - V_{0_\omega}) \cdot m \cdot t \cdot n \quad (26)$$

Eq. (26) is the expression of Fig.2.

2 Physical design

2.1 Structure of the gasflow style level posture sensor

As shown in Fig.3, the gasflow style level posture sensor consists of a hermetic chamber, a thermal resistance wire, and other mechanical parts. The sense element is constituted by the two independent cylinders which form a hermetic chamber, and the two components are connected in the middle by a screw. With this conformation the two reciprocal interferences of gas in two chamber's interior are avoided easily, and the measured precision is improved. Because the two chambers correspond to the plus and minus axials respectively, the dimension of the two chamber parts is the same to keep the consistency of the plus and minus axials. In the electric circuit, the left chamber of two thermal resistance wires is in series with the right chamber of two thermal resistance wires, as the thermal and sample resistance (as r_1, r_2 in Fig.3). This kind of connection of the two thermal resistance wires increases resistance. So under the same input voltage, the gyroscope's stability is improved because the electric current of thermal resistance wire is decreased; also the gyroscope's precision is improved.

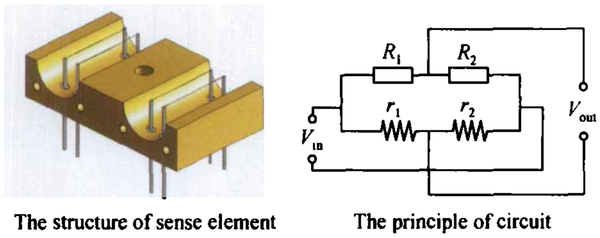

Fig. 3. The structure of the gasflow style tilt.

2.2 Structure design of the gasflow style angular velocity gyroscope

As shown in Fig. 4, the sense element of the gasflow style angular velocity gyroscope mainly consists of a cover, adjusting key, plate reed, pump pedestal, pump shelf, piezoelectricity pump, heating sense stopper, spray system, spray head, and shell. The spray system consists of two cylinders with different diameters. The middle of the spray system is the gasflow chamber.

2.3 Design of the signal processing circuit

The block diagram of the signal processing circuit is shown in Fig. 5. Based on the output characteristics of the gasflow style tilt and the angular velocity gyroscope, we have designed the following optimized signal processing electric circuit.

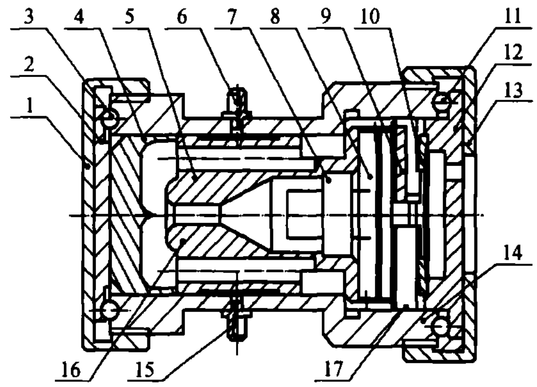

Fig. 4. The sense part of the gasflow type angular velocity gyroscope. 1, Small nut; 2, small clamp; 3, small seal ring; 4, end cover; 5, body of nozzle; 6, inlet valve; 7, sensitive plug; 8, pump bracket; 9, pump block; 10, dish spring; 11, big seal ring; 12, large clamp; 13, big nut; 14, shell; 15, gas outlet valve; 16, nozzle; 17, navigation key.

(i) Using the flatpacks device and the high accuracy MCU, we can gain singal data compensation from the bridge sampling circuit directly. This technique substitutes the signal amplifying circuit, the filter and the compensating circuit. The space of the signal processing circuit is reduced greatly, and two circuit boards are reduced to one, so the sensor volume is reduced nearly to 2/3 of the original one.

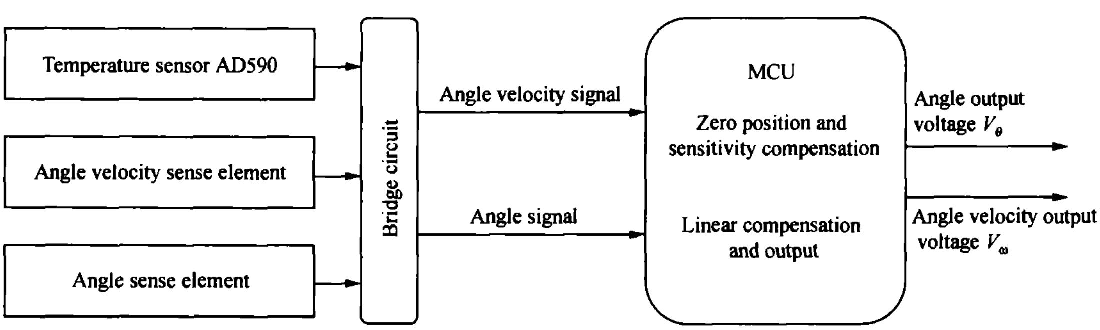

Fig. 5. The signal processing circuit frame of the gasflow style assembled inertial sensor.

(ii) Instead of the conventional circuit, the new circuit composed of the Silicon Lab's C8051F350 MCU and the temperature sensor compensates out inertial measurement system. This not only overcomes the difficulties in traditional hardware simulation compensating process and reduces the cost, but also enhances the compensate effect.

3 Signal processing technology

3.1 MCU compensation

In order to enhance the performance of the sensor, we must compensate the zero position voltage temperature, sensitivity temperature and non-linearity. Without affecting the sensor's response speed and resolution, we used the motion type arithmetic method of average to process data acquisition, and the non-scalar spacing partition polynomial fitting method, the conic section fitting formula, the linearity interpolation and a high precision device MCU C8051F350 were applied to compensate respectively the zero position voltage temperature, sensitivity temperature, non-linearity and symmetry. Fig. 6 shows the MCU compensation flow chart.

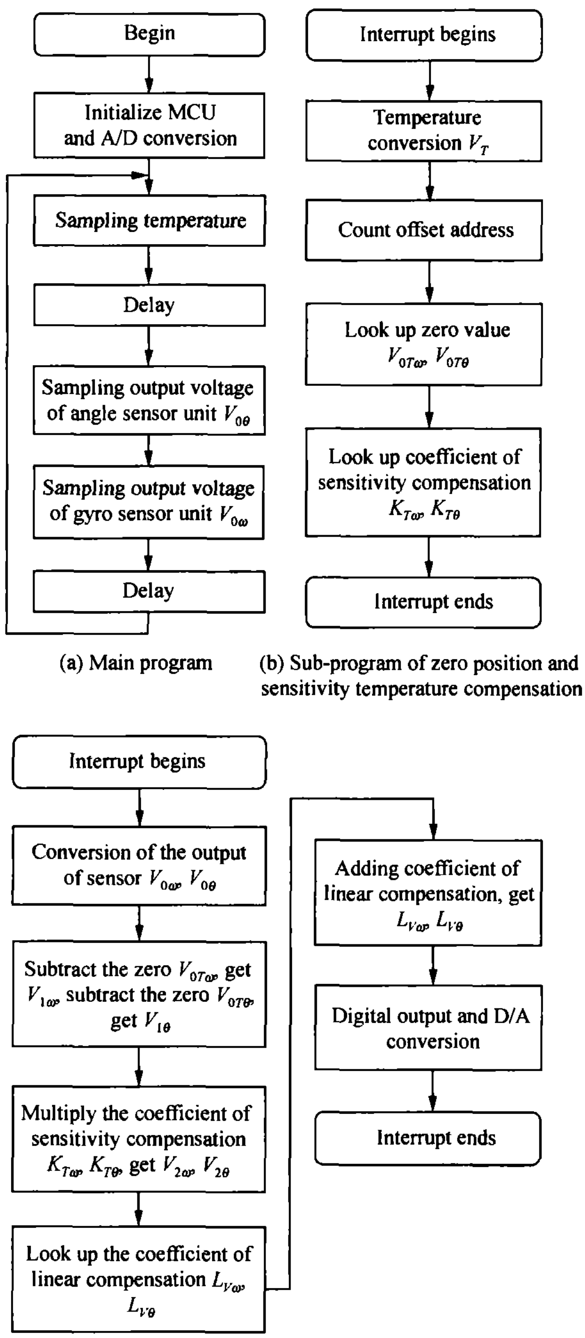

(a) Main program (b) Sub-program of zero position and sensitivity temperature compensation

(c) Sub-program of linearity compensation and output

Fig. 6. Flow chart of MCU compensation.

3.1.1 Zero position compensation program

(i) Sampling the zero position output voltage through various temperatures of the sensitive unit.

(ii) Using the multinomial stimulant curve formula, the output temperature of receptive points' zero position voltage can be calculated. And the zero position-temperature parameter is established.

(iii) Sampling the output voltage of diode sensor unit V_T, and by checking parameter list we can get the zero position value $V_{0T\omega}$ of the gyroscope sensor device and the zero position value $V_{0T\theta}$ of the gesture sensor device.

(iv) Subtracting receptive $V_{0T\omega}$ and $V_{0T\theta}$, from $V_{0\omega}$ and $V_{0\theta}$, we can get the output voltage of zero position compensation $V_{1\omega}$ and $V_{1\theta}$. The performance of $V_{1\omega}$ and $V_{1\theta}$, which has been changed with temperature after compensation, will exceed the sensor's final performance requirement.

3.1.2 Temperature sensitivity compensation program

(i) After zero position compensation, we put the flat attitude sensor in a high thermostat according to its measured maximum value, then sampling the output values at various temperatures of the sensitive unit. After the temperature stabilized, the sensor was taken out rapidly, and put on a turntable, it revolved according to the measured maximum value, and the output values at various temperatures for the sensitive unit were collected.

(ii) Using the conic section fitting formula and the linearity interpolation method, we can calculate the amplifier coefficient at every temperature point in the range of working temperature and establish the sensitivity compensation coefficient-temperature parameter list.

(iii) By sampling the output voltage of diode sensor unit V_T, checking the parameter list, we get the sensitivity compensation value $K_{T\omega}$, $K_{T\theta}$ at this temperature point.

(iv) Using $V_{1\omega}$ and $V_{1\theta}$ to multiply $K_{T\omega}$, $K_{T\theta}$, we will get the output voltage of sensitivity compensation $V_{2\omega}$, $V_{2\theta}$.

3.1.3 Nonlinear compensation program

(i) Testing the sensor's angular speed analogy voltage $V_{2\omega}$ and the bevel analogy voltage $V_{2\theta}$, we get the nonlinear compensation interpolation table.

(ii) Using the nonlinear compensation interpolation table, through linearity interpolation method, we get the actual compensation value of angular rate voltage LV_ω and bevel voltage LV_θ.

(iii) Using add or subtract processing, we get the sensor's final outputs V_ω, V_θ.

3.2 Comparison of the performance

When using such a software compensation method, the zero position voltage temperature, temperature sensitivity and the linearity of sensor have been improved greatly, and the operating temperature range has been expanded. The sensor's outputs with or without the compensation are shown in Fig. 7—Fig. 12. The sensor's nonlinearity declines from $\leqslant 2\%$ to $\leqslant 0.5\%$; sensitivity variety declines from $\leqslant 15\%$ to $\leqslant 0.6\%$; operating temperature range expands from $-10℃$—$+40℃$ to $-45℃$—$+55℃$.

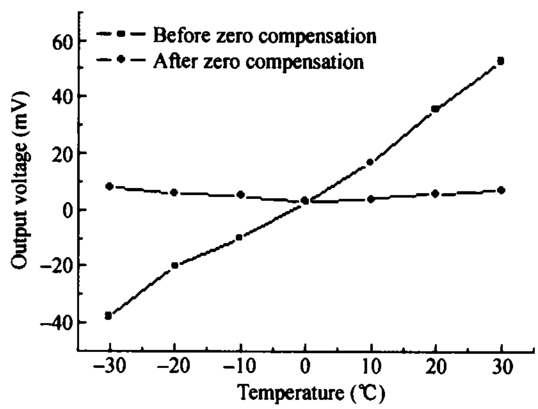

Fig. 7. The zero position voltage compensation of the gasflow style level posture sensor.

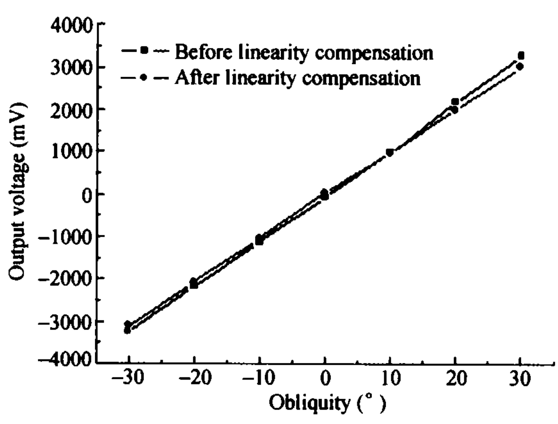

Fig. 8. The linear compensation of the gasflow style level posture sensor.

4 The ability of restraining acceleration interfere

The assembled gasflow style inertial sensor was placed on the vibration table, taper block and rotating table separately, and the ability of restraining interference acceleration was measured at line vibration, angle vibration and sway vibration.

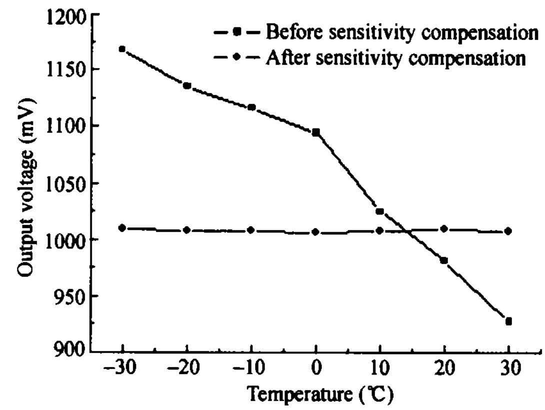

Fig. 9. The sensitivity compensation of the gasflow style level posture sensor.

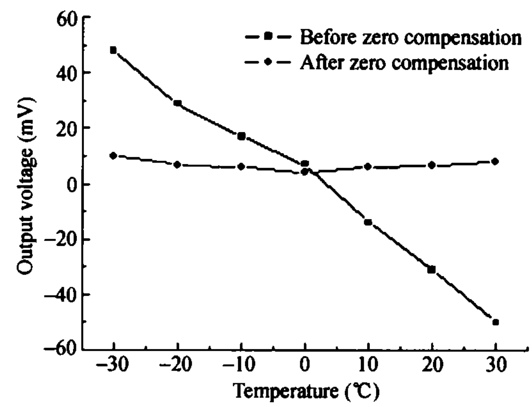

Fig. 10. The zero position voltage compensation of the gasflow style angular velocity (tilt angle 10°).

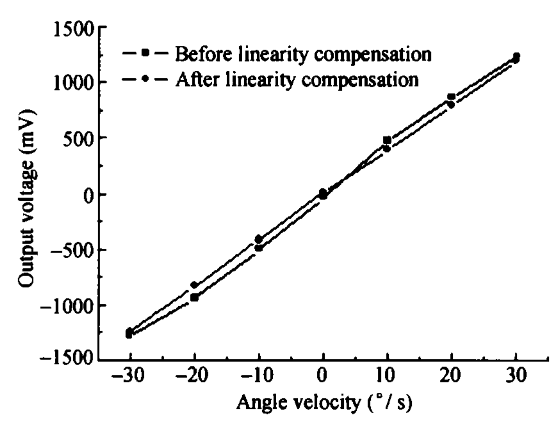

Fig. 11. The linearity compensation of the gasflow style angular velocity.

4.1 Line vibration

The assembled gasflow style inertial sensor and the gasflow style level posture sensor were placed on the vibration table. The wave patterns of the sensors are shown in Fig. 13 at a tilt angle 10°, frequency 12 Hz, displacement 0.75 mm and vibration interference acceleration 0.2 g. The gasflow style level posture

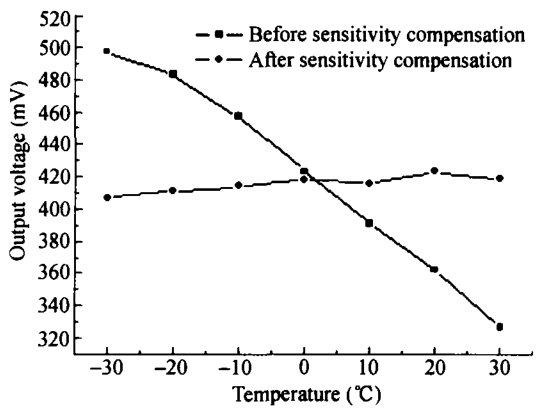

Fig. 12. The sensitivity compensation of the gasflow style angular velocity (tilt angle 10°).

sensor produced an interference signal of peak to peak value 600 mV because of the vibrating interfere acceleration, but the assembled gasflow style inertial sensor output signal value stayed nearly constant at 1.5 V because of the restraining interference acceleration.

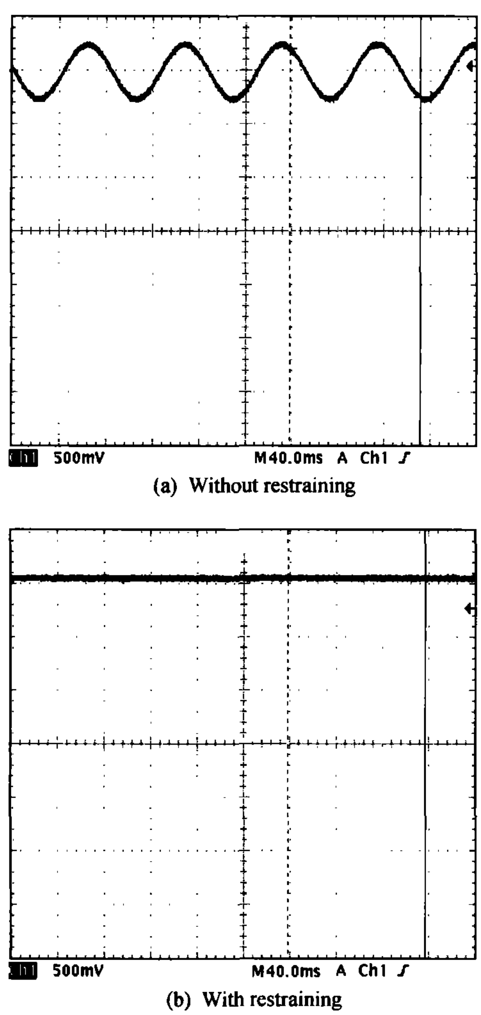

Fig. 13. The ability of the gasflow style assemble inertial sensor at line vibration.

4.2 Angle vibration

The assembled gasflow style inertial sensor and the gasflow style level posture sensor were placed on the taper block at a tilt angle 10°. The wave patterns of the sensors are shown in Fig. 14. Fig. 14 (a) shows that the gasflow style level posture sensor produces an excessive interference signal of 200 mV for the vibrating interference acceleration, but the inertial sensor has not this excessive signal for the restraining interfere acceleration.

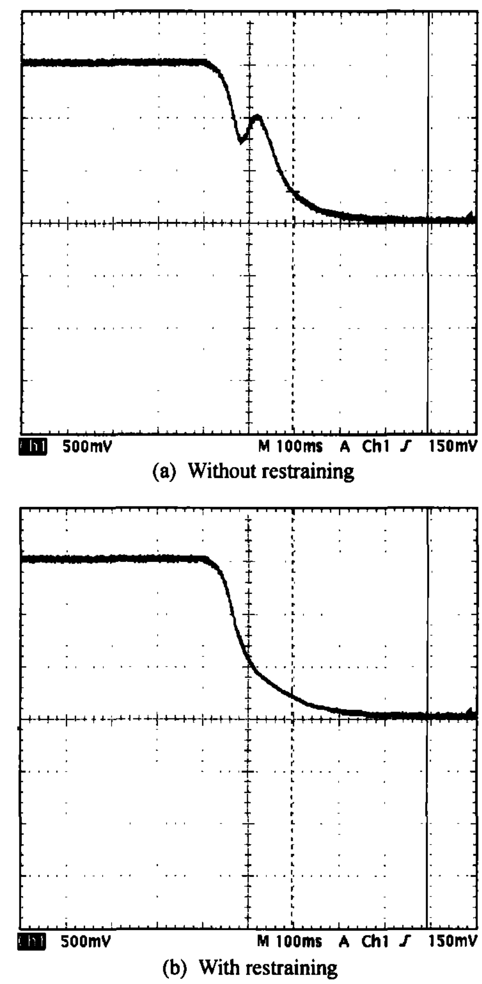

Fig. 14. The ability of the gasflow style assemble inertial sensor at angle vibration.

4.3 Sway vibration

The two above-mentioned sensors were placed on the HE type rotating table with two axies at the angle velocity of 30°/s in a come-and-go way. The output curves of the sensors are shown in Fig. 15. From Fig. 15(a), it can be seen that the gasflow style level posture sensor produces many interference signals, the peak value reaches 5 V because of the vibrating interference acceleration, but the assembled gasflow style inertial sensor has an interference signal of 8 mV because interference acceleration was suppressed. Therefore the anti-interference ability of the latter is much stronger.

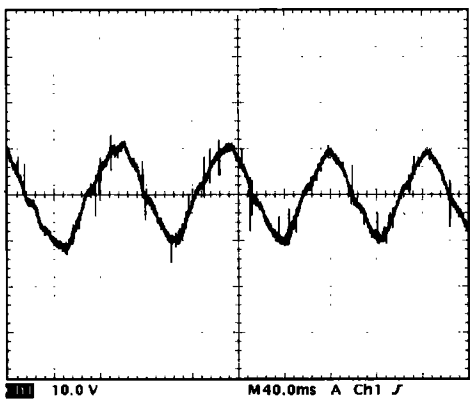

(a) Without restraining

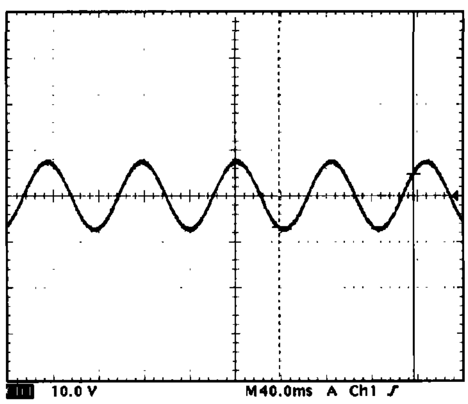

(b) With restraining

Fig. 15. The anti-interference ability of the assembled gasflow style inertial sensor at sway vibration.

5 Conclusions

(i) The compensation loop is composed of the gasflow style level posture sensor and the angular velocity gyroscope. The gyroscope sensor's output signal can suppress the effect brought by acceleration interfere restrain on the level posture sensor. Therefore, the assembled gasflow style inertial sensor can sense the plane gesture of moving carriers.

(ii) The MCU device was used to compensate the zero position voltage, temperature sensitivity and non-linearity. It widened the sensor's working temperature range and improved the linearity greatly.

References

1 Warren MR, Games PH and Ejup NG. Handbook of Heat Transfer Fundamentals. 2nd ed. New York: McGraw-Hill, 1985

2 Yu B, Chen YX and Guo XZ. Inertial Technology (in Chinese). Beijing: Publishing House of Beijing, 1994

3 Zhang FX. The Accelerometer and tilt sensor based on natural convection gas pendulum. In: Proceedings of 2004 International on Information Acquisition. HeFei, China, 2004, 122—125

4 Zhang FX. Gas pendulum acceleration sensor. Chinese Journal of Electronics, 2000, 9(1): 16, 64

5 Zhang FX. Natural convection gas pendulum and its application in accelerometer and tilt sensor. Progress in Natural Science, 2005, 15(9): 857—860